Calculation of water/air stopping-power ratios using EGS4 with explicit treatment of electron-positron differences

C. Malamut,[a] D. W. O. Rogers, and A. F. Bielajew
Institute for National Measurement Standards, National Research Council Canada, Ottawa K1A 0R6, Canada

(Received 14 November 1990; accepted for publication 21 June 1991)

Using the EGS4 Monte Carlo simulation program, a general purpose code has been written to calculate Bragg–Gray and Spencer–Attix stopping-power ratios for use in radiation dosimetry. The stopping-power ratios can be calculated in any material in any region in a general cylindrical geometry with a large number of source geometries possible. The calculations take into account for the first time the differences between the stopping powers and the inelastic scattering of positrons and electrons. The results show that previous calculations ignoring these effects were accurate. The present results agree, typically within 0.1%, with the Spencer–Attix water-to-air stopping-power ratios for broad parallel beams of electrons given in the AAPM and IAEA protocols except at the surface where the present calculations follow the buildup of secondary electrons in more detail and see a 2% reduction in the stopping-power ratios.

I. INTRODUCTION

Electron stopping-power ratios play a central role in radiation dosimetry because they are used in Spencer–Attix cavity theory to relate the dose in one medium to the dose in the surrounding medium, i.e.,

$$\frac{D_m}{D_g}=\left(\frac{\bar{L}}{\rho}\right)_g^m=\frac{\int_\Delta^{E_{\max}}\Phi_T[L(\Delta)/\rho]_m\,dE+TE_m}{\int_\Delta^{E_{\max}}\Phi_T[L(\Delta)/\rho]_g\,dE+TE_g}, \quad (1)$$

where m and g are the two media, Φ_T is the fluence spectrum of primary and secondary charged particles (i.e., $\Phi_T\,dE$ is the number of charged particles per unit area with energies between E and $E+dE$), Δ is low-energy cut-off below which all electrons are considered to deposit their energy locally, $[L(\Delta)/\rho]_{\text{med}}$ is the restricted collision stopping power in medium med for energy losses below Δ and TE is a track-end term to take into account charged particles falling below Δ. This equation assumes that electrons with energy below Δ are absorbed on the spot and that the cavity does not affect the charged-particle fluence spectrum Φ_T.

Stopping-power ratios appear in two central equations in radiation dosimetry. The most important is the equation for the dose to a medium given the charge measurement from an ion chamber when the medium is irradiated by a photon or electron beam, viz,

$$D_{\text{med}}=MN_{\text{gas}}\,(\bar{L}/\rho)_{\text{air}}^{\text{med}}P_{\text{ion}}P_{\text{repl}}P_{\text{wall}}\quad(\text{Gy}), \quad (2)$$

where M is the charge from the ion chamber corrected to standard conditions, N_{gas} is the cavity gas calibration factor and the three P factors are corrections which appear in the AAPM dosimetry protocol.[1] A stopping-power ratio also appears in the basic equation for determining exposure based on measuring charge from an ion chamber, viz.,

$$X=\frac{Q_{\text{gas}}}{m_{\text{air}}}\left(\frac{\bar{L}}{\rho}\right)_{\text{air}}^{\text{wall}}\left(\frac{\overline{\mu_{\text{en}}}}{\rho}\right)_{\text{wall}}^{\text{air}}K_hK\quad(\text{C/kg}), \quad (3)$$

where Q_{gas} is the charge liberated in an ion chamber exposed in a ^{60}Co beam, m_{air} is the mass of dry air in the chamber, $\left(\overline{\mu_{\text{en}}}/\rho\right)_{\text{wall}}^{\text{air}}$ is the ratio of mass energy absorption coefficients for air and the wall material and the K's are various correction factors. This equation plays a central role in determining the cavity-gas calibration factor N_{gas} used in various protocols.

ICRU Report 35 contains a full discussion of the calculation of stopping-power ratios.[2] Several authors have reported extensive series of calculations for use in radiation dosimetry. For electron beams, Berger and Seltzer of NIST were the leaders in the field.[2,3] Their values are based on extensive Monte Carlo calculations with ETRAN to obtain the electron fluence spectrum Φ_T. The resulting stopping-power ratios are used for electron beams in the AAPM and IAEA protocols.[1,4] Nahum[5] made a significant step forward by recognizing the importance of the track-end term in Eq. (1) and in using Monte Carlo calculations for photon beams. Nonetheless the photon stopping-power ratios used in the AAPM protocol are based on Cunningham and Schulz's analytic calculations of Φ_T.[6] Andreo and Brahme[7] have done extensive Monte Carlo calculations for photon beams and their results are used in the IAEA and other protocols.[4]

In all of the Monte Carlo calculations mentioned above, the codes consider positrons to be the same as electrons except that they produce two 511-keV photons when they annihilate. This is an approximation because electrons and positrons interact differently in matter and in particular their collision stopping powers are considerably different as is shown in Fig. 1. They also scatter differently and their radiative stopping powers are somewhat different.[8] For high-energy photon beams on water phantoms, pair production plays an important role. For example, positrons are 25% of the charged-particle fluence created by 20-MeV photons. One might expect that stopping-power ratios calculated with electrons and positrons treated separately would be different from those in which they were treated as the same.

To investigate this effect, the EGS4 code has been used to calculate charged particle fluence spectra and a code has been developed to calculate the stopping-power ratios. The paper starts by describing an EGS4 user code, called

 0094-2405/91/061222-07$01.20

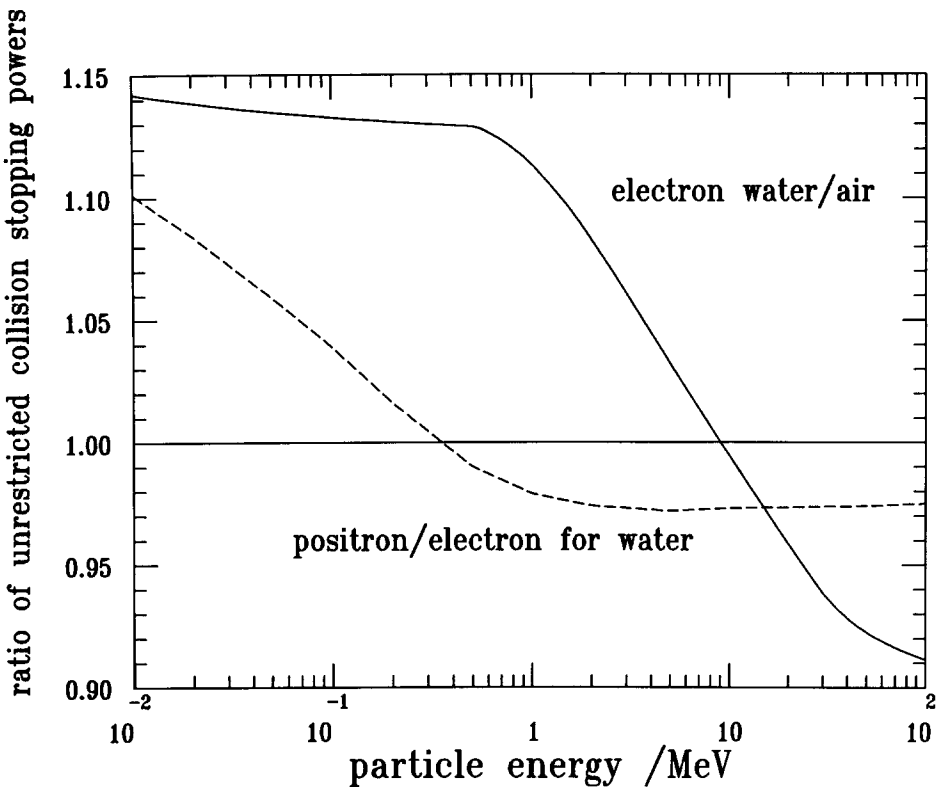

FIG. 1. Ratio of positron to electron unrestricted collision stopping powers in water as a function of energy and the ratio of water-to-air electron unrestricted collision stopping powers. Data based on ICRU Report 37.[8]

FLURZ, and the code SPR used to calculate the stopping-power ratios. To demonstrate that FLURZ and SPR work, a comparison is made of our results for electron beam stopping-power ratios to those calculated using other codes. A comparison to other photon beam calculations shows that explicit treatment of positrons makes no significant difference to the values of Spencer–Attix stopping-power ratios in water.

II. THE EGS4 USER CODE FLURZ

EGS4 is a widely used general purpose package for doing Monte Carlo simulations of electron and photon transport in materials[9] and has been extensively benchmarked in many situations.[10,11] EGS4 keeps track of electrons and positrons separately. For positrons it uses the appropriate collision stopping power, treats inelastic scattering from electrons using the Bhabha scattering cross section instead of the Moller cross section and simulates annihilation in flight. It has been shown that these differences can make up to a 5% difference in the peak dose per unit incident fluence in positron beams compared to electron beams of the same energy[12] and a 13% difference in the calculated germanium detector full-energy peak efficiency for positrons compared to electrons.[13] EGS4 makes the approximations that elastic multiple scattering and bremsstrahlung radiation are the same for positrons as for electrons. Use of these approximations should have no effect in calculations of stopping-power ratios.

The PRESTA electron transport algorithm was used with the EGS4 system in order to save computing time.[14] In applying PRESTA in this application a coding error was found in the PRESTA routine which leads to a small but distinct error when scoring fluence. (The error was that, contrary to the documentation, the PRESTA algorithm used the energy near the beginning of the step to evaluate various quantities needed during each step. It should be the middle of the step.)

The original fluence-scoring code developed at NRCC scored the fluence in a plane by doing a weighted count of the particles crossing the plane (see Ref. 15). This is very inefficient when scoring low-energy electrons and so FLURZ(V13) scores the total particle path length per unit volume. Chilton has formally proved that this quantity is equivalent to the average fluence in the volume.[16,17] The code works with a general cylindrically symmetric geometry with arbitrary materials in each region. An arbitrary input energy spectrum of electrons, positrons, or gamma-rays is handled in a total of ten or so different source geometries (broad parallel beams from the end or side of the cylinder, point sources, etc.). The code scores electron, photon, and positron fluence spectra (i.e., differential in energy) in each region of the geometry. The spectra can have energy bins that are: equal, arbitrary, equally spaced in the logarithm of the energy for the entire energy range, or with logarithmic energy bins except for the top 10% of the energy spectrum which is covered by 10% of the bins of equal width. This latter option proved to be the most convenient for calculating stopping-power ratios. The use of relatively small equal-energy bins near the maximum energy was found necessary in monoenergetic electron beams to avoid artifacts near the surface where the energy spread of the electrons can be much less than the logarithmic bin size. To make uncertainties due to bin-size artifacts negligible, this latter option was used with 150 bins although 75 or even fewer bins would probably do as well.

When using PRESTA, large step sizes can occur and in the scoring routine it was found essential to distribute the path length in each step across several energy bins. This was done assuming the electron stopping power was constant in the step. This approximation can become invalid for very large steps and so it was found necessary to restrict step sizes to maximum energy losses (ESTEPE) of 10% or less in order to score the pathlength properly. With larger steps, the higher stopping power at lower energies in the step (especially for low-energy electrons where the stopping power changes the most) implied less path length should be associated with the lower-energy electrons. Hence, use of excessively large steps with this simple scoring algorithm causes the fluence scored to be too large for the low-energy electrons.

For calculating Bragg–Gray stopping-power ratios the integrals are over the fluence spectra of primary charged particles only and hence it was necessary to score the fluence spectra for primary charged particles which were taken to include everything except knock-on electrons (i.e., charged particles created by phantom generated bremsstrahlung are included as primaries).

The stopping powers used by the EGS4 system[9] are close approximations of the ICRU report 37 values.[8] However, to eliminate any uncertainties (which can amount to 0.5%), a slightly modified version of the data preparation package was used which produces exactly the ICRU collision and radiative stopping powers[18,19] except that positron radiative stopping powers are taken to be the same as those for electrons.

In the calculations reported here, the value of Δ has been taken to be 10 keV as done in major protocols.[1,4] The fluence spectra have been calculated down to Δ using the Monte Carlo code.

Earlier versions of the FLURZ code have been used to calculate stopping-power ratios[20,21] but the changes described above represent a fine tuning of the code for the present application. After this paper was submitted, an extensive paper was published that used EGS4 to calculate electron beam stopping-power ratios.[22] With minor exceptions there is good agreement with the present results for electron beams except at the surface where large depth bins were used.

III. THE SPR CODE

The code SPR takes electron and positron fluence spectra and calculates the stopping-power ratios given by Eq. (1), again explicitly accounting for the differences in the electron and positron stopping powers. The track-end term is given by $\Phi_T(\Delta)[S(\Delta)/\rho]_{\text{med}}\Delta$.[2,5] The collision stopping-power data are from the EGS4 data files prepared by PEGS4. The stopping-power ratios could be calculated for any two media but the usual application is for the material in the numerator to be that for which the fluence spectrum was calculated and for the material in the denominator to be that of the detector (usually air).

The integral is approximated by a summation over the energy bins. The energy of each bin was taken as its midpoint which is accurate as long as the fluence and stopping powers vary linearly across the bin. This was verified when using 150 bins because the calculated stopping-power ratios using the midbin energies were the same as the average of those calculated using the energies at the beginning and end of the bins (which differed by up to $\pm$ 0.3% from the average).

Bragg–Gray stopping-power ratios are calculated from an equation similar to Eq. (1) but using the primary charged-particle fluence instead of the total fluence, the unrestricted collision stopping power instead of the restricted stopping power and with no track-end term. Strictly speaking the integral over energy extends to zero but the fluence of primaries below Δ is completely negligible.

The track-end term was found to contribute between 5% and 10% to the dose in many situations, but it typically had an effect of 0.5% to 1% on the calculated water-to-air stopping-power ratios for electrons in a water phantom. As done by Nahum, one of the checks of the code was to evaluate the numerator separately and verify that it was the same as the dose calculated by scoring energy deposition directly in the Monte Carlo code.[5,21]

IV. COMPARISON TO PREVIOUS ELECTRON BEAM RESULTS

Figure 2 compares Spencer–Attix stopping-power ratios calculated with the present code to those calculated by Berger for the AAPM protocol.[1,3] Away from the surface the agreement is remarkable, typically within 0.1% except at depths greater than 10 cm in the 50-MeV beam where the present results are up to 0.3% less than the previous results. This generally good agreement is surprising since an error has been found in the ETRAN code which Berger used to calculate these stopping-power ratios.[23,24] The error led to 8% to 10% underestimates of the absorbed dose at depths shallower than $d_{\max}$ but clearly has no significant effect on the stopping-power ratios except possibly in the 50-MeV beam.

Away from the surface, the Bragg–Gray stopping-power ratios are a few (typically 4 or 5) tenths of a percent less than the Spencer–Attix values over a broad range of depths. The present results are not completely consistent with those of either Berger *et al.*[3] or Nahum[5] who predict differences of up to 1% although they are in better agreement with Nahum's more recent calculations.[21] However, Nahum has shown these differences are strongly linked to the relative mean ionization values used to calculate the stopping powers of the two materials involved[21] and hence the differences seen here may only reflect differences in the I-values used. In the case of 10-MeV electrons on an aluminum phantom the present calculations give a 2.4% difference between the Spencer–Attix and Bragg–Gray results at a depth of 0.4–0.5 r_0, which differs somewhat from the 3.0% difference reported by Nahum.[21]

Figure 3 shows the detail of the calculated stopping-power ratios at the water surface in a 20-MeV electron beam. At the surface, charged-particle equilibrium of the secondary electrons does not exist. However, Bragg–Gray stopping-power ratios are based on the assumption that there is complete secondary charged particle equilibrium, even at the phantom surface and hence the Bragg–Gray calculations break

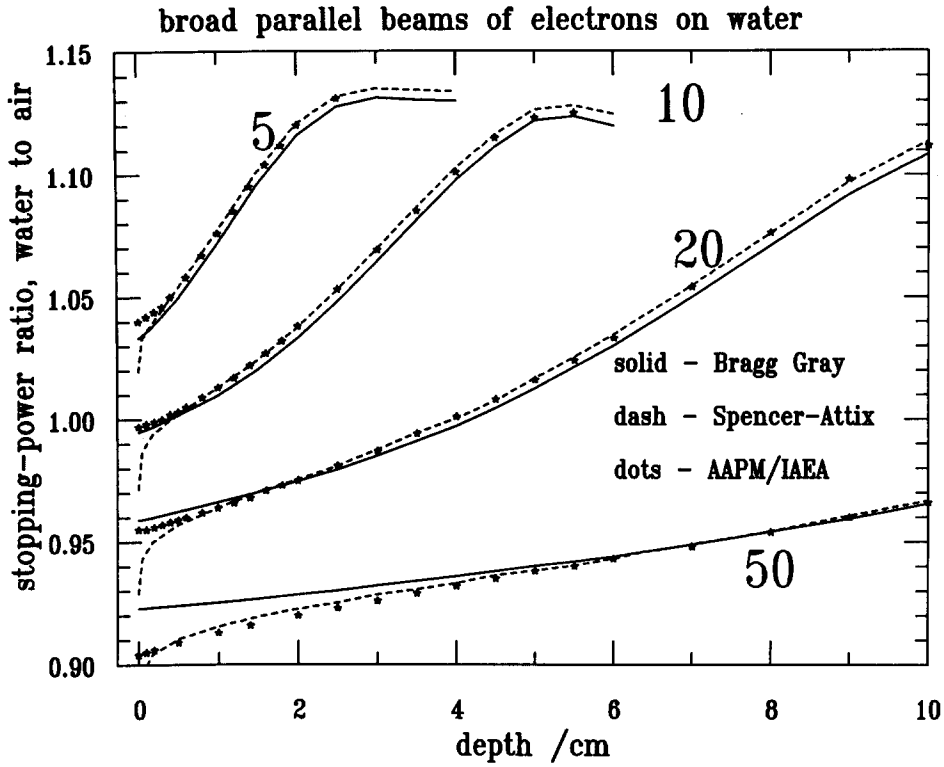

FIG. 2. Stopping-power ratios of water-to-air for broad parallel beams of 5-, 10-, 20- and 50-MeV electrons incident on a water phantom. The solid curves are the present Bragg–Gray stopping-power ratios, the dashed curves are the present Spencer–Attix calculations and the dots are Berger's results as quoted in the AAPM and IAEA protocols.[1,4]

down and are inaccurate at the surface. Figure 3 also shows a 2% discrepancy at the surface between the AAPM's Spencer–Attix stopping-power ratios and those calculated here. This occurs, at least partially, because Berger, in calculating the AAPM's stopping-power ratios only followed electrons down to $E_0/32$ using the Monte Carlo technique and generated the fluence spectra below this energy assuming charged particle equilibrium of the knock-on electrons held.[3] In both cases (i.e., the Bragg–Gray stopping-power ratios and the AAPM Spencer–Attix stopping-power ratios) the assumption at the surface of charged-particle equilibrium of knock-on electrons means the calculation includes an excess of low-energy electrons and as can be seen from Fig. 1, the higher ratio of water-to-air stopping powers

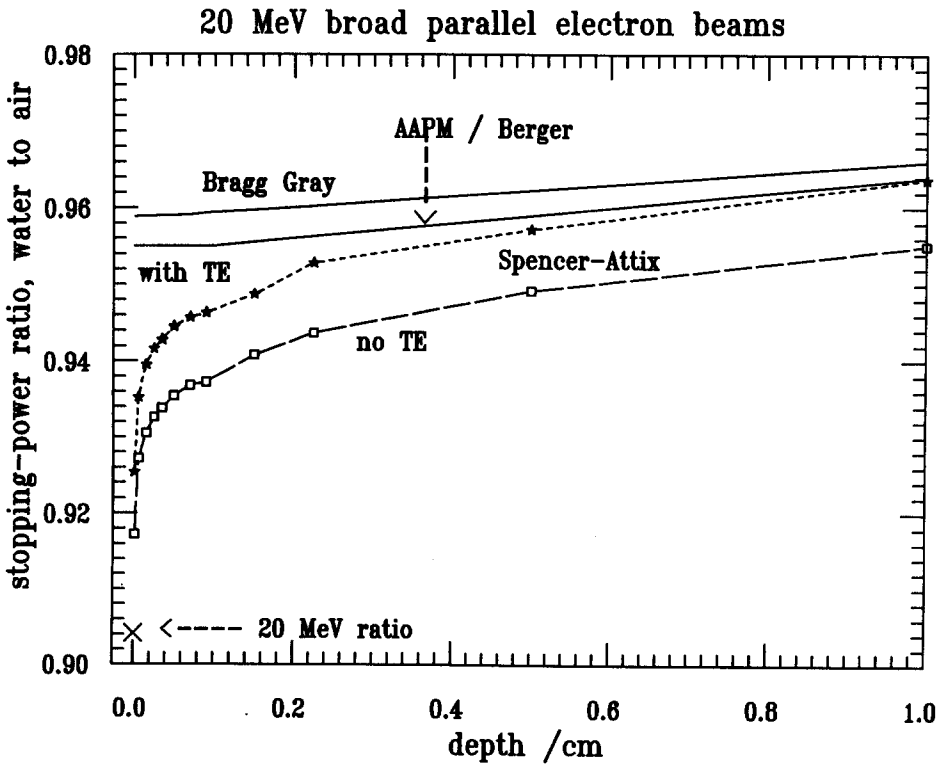

FIG. 3. Calculated water-to-air stopping-power ratios near the surface of a water phantom irradiated by a broad parallel beam of 20-MeV electrons. The upper curve is Bragg–Gray stopping-power ratios whereas all the other curves are for Spencer–Attix stopping-power ratios with $\Delta = 10$ keV. The lower solid curve is from the AAPM protocol;[1] the short dashes are the present calculations with track-ends, the long dashes without track-ends. The $\times$ symbol shows the ratio of stopping powers at 20 MeV. The ratio of unrestricted collision stopping powers at 20 MeV is 0.959, in good agreement with the Bragg–Gray stopping-power ratios at the surface.

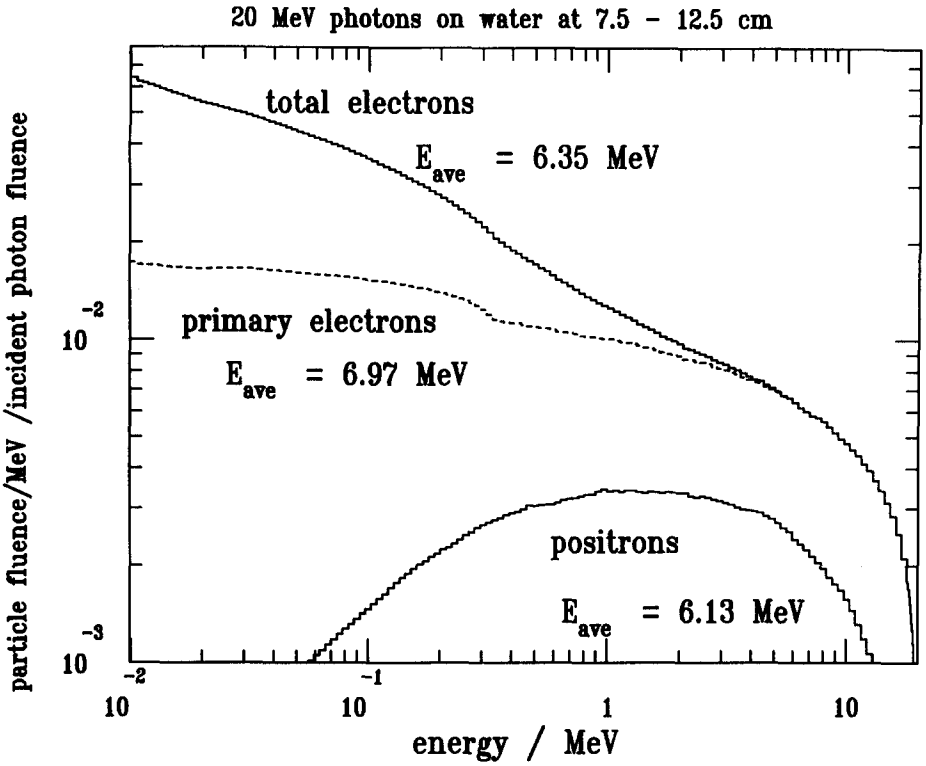

FIG. 4. Electron and positron fluence spectra between 7.5- and 12.5-cm depth in a water phantom irradiated by a broad parallel beam of 20-MeV photons. The electrons represent 78% of the charged particle fluence and the positrons the other 22%. The dashed curve shows the primary electron fluence.

for these excess low-energy electrons causes the stopping-power ratios to increase. These surface effects would also be washed out in any calculation using depth bins which were thick compared to the region of the effect.

At the surface, the correct stopping-power ratios are up to 2% less than given in the AAPM protocol. However, at least in a broad beam, 100 cm of air would be the equivalent of about 1 mm of water and hence the effect of the air above any realistic phantom would tend to minimize these buildup effects. The figure also shows the simple ratio of restricted collision stopping powers for monoenergetic 20-MeV electrons. It can be seen that at the surface the backscattered and secondary electrons increase the stopping-power ratios by about 2% above this value. Lastly, Fig. 3 shows the size of the track-end term which is about 1%.

V. PHOTON BEAM STOPPING-POWER RATIOS

Figure 4 presents the electron and positron fluence spectra at depths near 10 cm in a 20-MeV photon beam. The positrons represent roughly 1/4 of the charged-particle fluence and have slightly lower mean energies than the electrons. The lack of low-energy positrons is both because there are no low-energy secondary positrons and because there are few low-energy positrons created in pair production, unlike electrons which are created with very low energy by the Compton process.

Table I compares the present calculations of stopping-power ratios for a variety of monoenergetic photon beams with the results of Andreo and Brahme[7] and Nahum (quoted in Ref. 7). For the sake of the comparison, in this case the calculations were done using the electron stopping powers in ICRU Report 35 (Electron Dosimetry) rather than ICRU Report 37 on electron stopping powers as done above. The values of the Spencer–Attix stopping-power ratios agree within about 0.1% with the calculations of Andreo and Brahme and within 0.5% with Nahum's calculations despite the fact that the previous calculations treated positrons as electrons which annihilated at the end of their path whereas the EGS calculation treats them as separate entities. The agreement with the Bragg–Gray stopping-power ratios is almost as good except for the 40-MeV beam where the positron fluence is more significant.

To investigate further the effect of treating positrons and electrons differently, the code SPR (but not FLURZ) was modified to use electron stopping powers for the positrons as well as the electrons. This caused the Spencer–Attix stopping-power ratios to change by no more than 0.02%. The Bragg–Gray ratios were also unchanged at lower energies

TABLE I. Comparison of the present water-to-air stopping-power ratios to those calculated by Andreo and Brahme and Nahum (both quoted in Ref. 7) for broad parallel beams of monoenergetic photons on water at a depth of 10 cm for Andreo and Brahme and at a depth where charged-particle equilibrium exists for Nahum's and the present calculation. Electron stopping power data are from ICRU Report 35.

Photon energy (MeV)	Bragg–Gray			Spencer–Attix		
	AB	Nahum	EGS4	AB	Nahum	EGS4
1	1.133	1.132	1.132	1.135	1.134	1.136
5	1.102	1.097	1.101	1.107	1.102	1.107
10	1.075	1.072	1.074	1.079	1.077	1.079
20	1.043	1.041	1.042	1.047	1.046	1.046
40	1.002	1.012	1.007[a]	1.005	1.015	1.011[b]

[a] At depth of 15 cm, value at 10-cm depth is 0.999.
[b] At depth of 15 cm, value at 10-cm depth is 1.003.

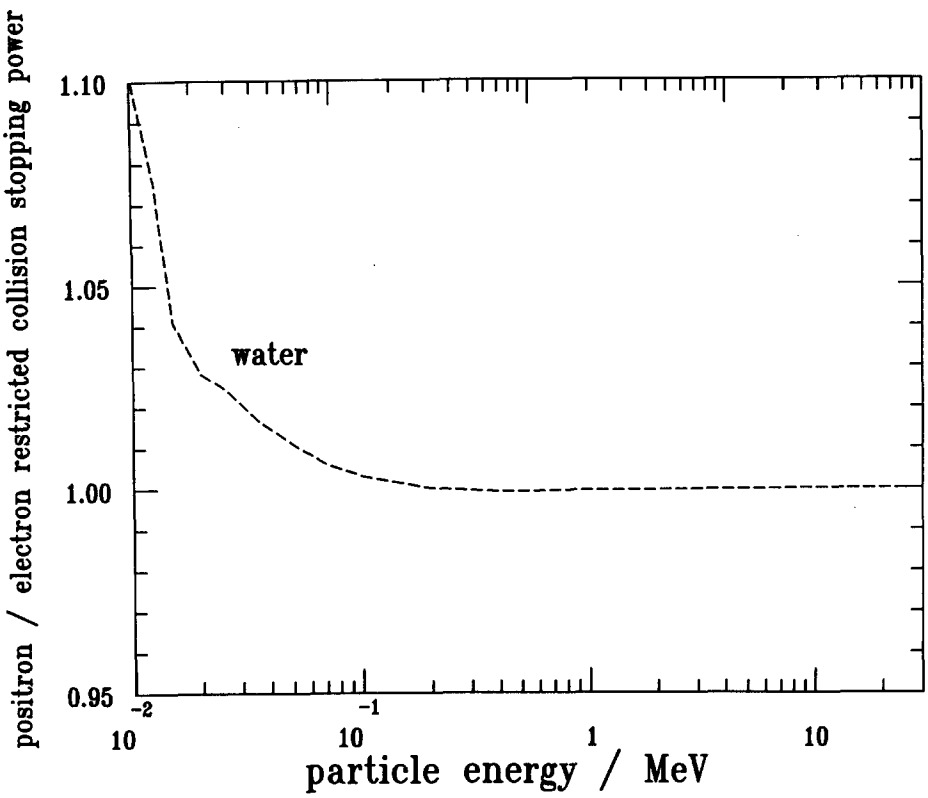

FIG. 5. Ratio of positron to electron restricted collision stopping powers ($\Delta = 10$ keV) in water as a function of energy. Data are based on Ref. 8.

but were 0.4% and 1.1% higher for the 20- and 40-MeV beams, respectively.

The lack of change when the electron restricted stopping powers were used instead of those for positrons is explained by Fig. 5 which shows that the ratio of positron to electron restricted collision stopping powers is essentially unity for all energies above 100 keV, unlike the ratio for unrestricted stopping powers which varies by 5% (see Fig. 1). The 10% variation in the ratio of restricted stopping powers below 100 keV has no effect on the stopping-power ratios which reflects the fact that there are so few positrons in this energy region as shown in Fig. 4.

The ratio of positron to electron stopping powers above 100 keV being unity reflects the fact that the entire difference in the unrestricted collision stopping powers comes from the differences in Bhabha and Moller scattering by which the positrons and electrons, respectively, lose energy while creating high-energy secondary electrons and there is virtually no difference in these cross sections for the production of low-energy secondary electrons.

VI. CONCLUSIONS

The EGS4 user code FLURZ(V13) has been shown to calculate particle fluence spectra which can be used as input to a second code, SPR, which calculates Spencer–Attix and Bragg–Gray stopping-power ratios which are in good agreement with previous calculations except where differences are expected, in particular near the surface.

The present results demonstrate that the Spencer–Attix stopping-power ratios show a buildup effect for knock-on electrons near the surface of a water phantom which other calculations do not predict because they do not follow electron transport to such low energies or in such narrow depth intervals. This comes at the expense of much greater computing time using the current approach and is of little practical importance because the air above any realistic phantom would create some buildup of secondaries.

The Spencer–Attix stopping-power ratios for photon beams calculated with codes that do not account for any differences between electrons and positrons slowing down have been shown to agree very well with the more accurate model used here although the formalism still ignores potential differences between $(W/e)_{air}$ for electrons and positrons (Nahum, private communication). There may be a small error for Bragg–Gray stopping-power ratios in high-energy beams calculated without keeping track of the differences between electrons and positrons, but these are expected to be less than 1% in monoenergetic high-energy photon beams, and much less in realistic clinical photon beams.

The statistical uncertainty on the calculated stopping-power ratios for broad parallel beams is small, typically better than 0.1% for calculations in which 10 000 electron histories are followed. This is consistent with the observations of Berger *et al.*[3] and Andreo and Fransson.[25]

ACKNOWLEDGMENTS

We wish to thank our NRCC colleague Carl Ross for his invaluable comments on the manuscript and acknowledge our debt of gratitude to our colleagues Alan Nahum of the Royal Marsden Hospital and Pedro Andreo of the Karolinska Institute who have taught us a great deal about the calculation of stopping-power ratios and also made helpful comments on the manuscript.

[a] Permanent address: Instituto de Radioproteção e Dosimetria, Rio, Brazil.

[1] AAPM, "A protocol for the determination of absorbed dose from high-energy photon and electron beams," Med. Phys. **10**, 741–771 (1983).

[2] ICRU Report 35, *Radiation Dosimetry: Electron Beams with Energies Between 1 and 50 MeV* (International Commission on Radiation Units and Measurements, Bethesda, MD, 1984).

[3] M. J. Berger, S. M. Seltzer, S. R. Domen, and P. J. Lamperti, "Stopping-power ratios for electron dosimetry with ionization chambers," in *Biomedical Dosimetry* (IAEA, Vienna, 1975), pp. 589–609.

[4] IAEA, *Absorbed Dose Determination in Photon and Electron Beams; An International Code of Practice*, Tech. Rep. Series #277(IAEA, Vienna, 1987).

[5] A. E. Nahum, "Water/air Stopping-Power Ratios for Megavoltage Photon and Electron Beams," Phys. Med. Biol. **23**, 24–38 (1978).

[6] J. R. Cunningham and R. J. Schulz, "On the selection of stopping-power and mass-energy absorption coefficient ratios for high energy x-ray dosimetry," Med. Phys. **11**, 618–623 (1984).

[7] P. Andreo and A. Brahme, "Stopping-power data for high-energy photon beams," Phys. Med. Biol. **31**, 839 (1986).

[8] ICRU Report 37, *Stopping Powers for Electrons and Positrons* (ICRU, Washington, DC, 1984).

[9] W. R. Nelson, H. Hirayama, and D. W. O. Rogers, *The EGS4 Code System*, Stanford Linear Accelerator Center Report SLAC-265 (Stanford, CA, 1985).

[10] D. W. O. Rogers and A. F. Bielajew, "Experimental benchmarks of EGS," in *Monte Carlo Transport of Electrons and Photons Below 50 MeV*, edited by W. R. Nelson, T. M. Jenkins, A. Rindi, A. E. Nahum, and D. W. O. Rogers (Plenum, New York, 1989), pp. 307–322.

[11] D. W. O. Rogers and A. F. Bielajew, "Monte Carlo techniques of electron and photon transport for radiation dosimetry," in *The Dosimetry of Ionizing Radiation*, edited by K. R. Kase, B. E. Bjarngard, and F. H. Attix (Academic, New York, 1990), Vol. III, pp. 427–539.

[12] D. W. O. Rogers, "Fluence to Dose Equivalent Conversion Factors Calculated with EGS3 for Electrons from 100 keV to 20 GeV and Photons from 20 keV to 20 GeV," Health Phys. **46**, 891–914 (1984).

[13] D. W. O. Rogers, "Low Energy Electron Transport with EGS," Nuclear Instruments Methods A **227**, 535–548 (1984).

[14] A. F. Bielajew and D. W. O. Rogers, "PRESTA: The Parameter Reduced Electron-Step Transport Algorithm for Electron Monte Carlo Transport," Nuclear Instruments Methods B **18**, 165–181 (1987).

[15] J. C. Cunningham, M. Woo, D. W. O. Rogers, and A. F. Bielajew, "The Dependence of Mass Energy Absorption Coefficient Ratios on Size and Depth in a Phantom," Med. Phys. **13**, 496–502 (1986).

[16] A. B. Chilton, "A Note on the Fluence Concept," Health Phys. **34**, 715–716 (1978).

[17] A. B. Chilton, "Further Comments on an Alternative Definition of Fluence," Health Phys. **35**, 637–638 (1979).

[18] S. Duane, A. F. Bielajew, and D. W. O. Rogers, "Use of ICRU-37/NBS Collision Stopping Powers in the EGS4 System," NRCC Rep. PIRS-0177, Ottawa, March 1989.

[19] D. W. O. Rogers, S. Duane, A. F. Bielajew, and W. R. Nelson, "Use of ICRU-37/NBS Radiative Stopping Powers in the EGS4 System," NRCC Rep. PIRS-0177, Ottawa, March 1989.

[20] D. W. O. Rogers, A. F. Bielajew, and A. E. Nahum, "Ion Chamber Response and A_{wall} Correction Factors in a ^{60}Co Beam by Monte Carlo Simulation," Phys. Med. Biol. **30**, 429–444 (1985).

[21] A. E. Nahum, "Extension of the Spencer–Attix Cavity Theory to the 3-media situation for electron beams," in *Dosimetry in Radiotherapy*, (IAEA, Vienna, 1988), Vol. I. pp. 87–115.

[22] P. Andreo, "Depth-dose and stopping-power data for mono-energetic electron beams," Nucl. Inst. Meth. B **51**, 107–121 (1990).

[23] D. W. O. Rogers and A. F. Bielajew, "Differences in electron depth-dose curves calculated with EGS and ETRAN and improved energy-range relationships," Med. Phys. **13**, 687–694 (1986).

[24] S. M. Seltzer, "An Overview of ETRAN Monte Carlo Methods," in *Monte Carlo Transport of Electrons and Photons Below 50 MeV*, edited by W. R. Nelson, T. M. Jenkins, A. Rindi, A. E. Nahum, and D. W. O. Rogers (Plenum, New York, 1989), pp. 153–182.

[25] P. Andreo and A. Fransson, "Stopping-power ratios and their uncertainties for clinical electron beam dosimetry," Phys. Med. Biol. **34**, 1847–1861 (1989).